SCIENTIFIC REPORTS

OPEN

SUBJECT AREAS:
LASERS, LEDS AND LIGHT SOURCES
OPTICAL MATERIALS AND STRUCTURES
ELECTRONIC PROPERTIES AND MATERIALS
APPLIED PHYSICS

Received
23 June 2014

Accepted
2 October 2014

Published
23 October 2014

Correspondence and requests for materials should be addressed to J.-J.S. (jjshi@pku.edu.cn)

Reducing Mg Acceptor Activation-Energy in $Al_{0.83}Ga_{0.17}N$ Disorder Alloy Substituted by Nanoscale $(AlN)_5/(GaN)_1$ Superlattice Using Mg_{Ga} δ-Doping: Mg Local-Structure Effect

Hong-xia Zhong[1], Jun-jie Shi[1], Min Zhang[2], Xin-he Jiang[1], Pu Huang[1] & Yi-min Ding[1]

[1]State Key Laboratory for Mesoscopic Physics and Department of Physics, Peking University, Beijing 100871, P. R. China, [2]College of Physics and Electron Information, Inner Mongolia Normal University, Hohhot 010022, P. R. China.

Improving *p*-type doping efficiency in Al-rich AlGaN alloys is a worldwide problem for the realization of AlGaN-based deep ultraviolet optoelectronic devices. In order to solve this problem, we calculate Mg acceptor activation energy and investigate its relationship with Mg local structure in nanoscale $(AlN)_5/(GaN)_1$ superlattice (SL), a substitution for $Al_{0.83}Ga_{0.17}N$ disorder alloy, using first-principles calculations. A universal picture to reduce acceptor activation energy in wide-gap semiconductors is given for the first time. By reducing the volume of the acceptor local structure slightly, its activation energy can be decreased remarkably. Our results show that Mg acceptor activation energy can be reduced significantly from 0.44 eV in $Al_{0.83}Ga_{0.17}N$ disorder alloy to 0.26 eV, very close to the Mg acceptor activation energy in GaN, and a high hole concentration in the order of 10^{19} cm^{-3} can be obtained in $(AlN)_5/(GaN)_1$ SL by Mg_{Ga} δ-doping owing to GaN-monolayer modulation. We thus open up a new way to reduce Mg acceptor activation energy and increase hole concentration in Al-rich AlGaN.

Al-rich AlGaN alloys are ideal materials for deep ultraviolet (DUV) optoelectronic devices with operating wavelength down to 200 nm due to their large direct band gaps[1–4]. They have potential applications in sterilization, water and air purification, biological and chemical agent detection, high-density data storage and medical research[5,6]. However, the external quantum efficiency of AlGaN-based DUV light-emitting diodes (LEDs) is extremely low around 0.1%[7,8]. Generally, three main factors, that is, the high dislocation density (10^{10} cm^{-2}), the low *p*-type doping efficiency, and the AlN-like valence-band maximum (VBM), i.e., the crystal-field split-off hole band as the VBM other than the heavy hole band (see Figure 2.12 in Ref. 9), contribute to this overall small value. We will here focus on improving *p*-type doping efficiency in Al-rich AlGaN. It is well-known that realizing *p*-type doping in Al-rich AlGaN is extremely difficult due to the following three major reasons, i.e., the high acceptor activation energy E_A, the compensation by nitrogen vacancies, and the limited acceptor solubility[9]. For the most widely used Mg acceptor dopant, its E_A increases monotonically with Al composition from 0.16–0.25 eV in GaN to >0.50 eV in AlN[9]. Therefore, realizing *p*-type Al-rich AlGaN has become one of the most challenging tasks in the nitride community.

Great efforts have been devoted to improve *p*-type conduction in group-III nitrides[10–16]. Polarization doping has been proposed to increase the hole concentration in compositionally graded AlGaN alloys, in which Mg acceptor is ionized by the polarization field[10–12]. Alternative acceptor-donor co-doping has also been developed to reduce the acceptor activation energy[13,14]. The non-equilibrium growing with pulse doping has been proved to increase the hole concentration[15]. Furthermore, Mg δ-doping, a impurity-growth mode by closing Ga and Al flow and leaving N and Mg flow, enhances the *p*-type conductivity of AlGaN alloys[16]. To the best of our knowledge, only several experiments are focused on the *p*-type conduction of Al-rich AlGaN alloys[3,9,17,18]. The related theoretical work is still absent at present. Our purpose here is to overcome the *p*-type doping bottlenecks in Al-rich AlGaN.

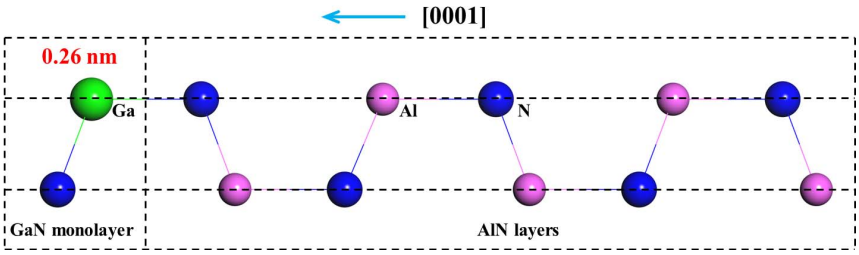

Figure 1 | Typical structural model of nanoscale $(AlN)_5/(GaN)_1$ SL with one GaN monolayer (0.26 nm).

We note that nanometer scale compositional inhomogeneity has an important influence on the luminescence efficiency of group-III nitride semiconductors[6,19–24]. It has been found that the nanoscale islands or quantum dots observed in AlGaN can improve its internal quantum efficiency[6,19,24,25]. Moreover, atomic-scale compositional superlattice (SL) has also been observed in Al-rich AlGaN thin films grown by molecular-beam epitaxy (MBE)[26]. Recent theoretical and experimental works prove that the nanoscale $(AlN)_m/(GaN)_n$ ($m > n$) SL, substituting for the Al-rich AlGaN disorder alloy, can convert the VBM from the crystal-field split-off hole to heavy hole band, which directly leads to the increase of the desired transverse electric (TE) polarized light emission efficiency in the DUV spectral region (Ref. 27 and Jiang, X.-h. *et al.*, unpublished data). Compared with Al-rich AlGaN alloy, the SL structure has an obvious advantage because it can combine the high TE polarized light emission efficiency of GaN and the wide energy gap of AlN.

According to the tight-binding approximation, we know that the electronic structures of Mg atom doped in AlGaN can be modified significantly by its nearest and next-nearest (NN) atoms. We will thus pay our attention to the nearest and NN atoms and investigate their influence on Mg electronic structures in nanoscale $(AlN)_5/(GaN)_1$ SL (see Figure 1) substitution for $Al_{0.83}Ga_{0.17}N$ disorder alloy. Our following results show that E_A decreases if the NN Ga-atom number increases and the Mg-centered tetrahedron volume decreases. The Mg acceptor activation energy can be reduced significantly to 0.26 eV, very close to the E_A of GaN, in $(AlN)_5/(GaN)_1$ SL by Mg_{Ga} δ-doping. A high hole concentration in the order of 10^{19} cm^{-3} can thus be obtained.

Results

In order to examine the stability of Mg doped structures, we first calculate the formation energy E^f of Mg acceptor in $(AlN)_5/(GaN)_1$ SL and $Al_{0.83}Ga_{0.17}N$ uniform alloy. Generally, E^f of a defect D in charge state q can be calculated as follows[28],

$$E^f[D(q)] = E_{tot}[D(q)] - E_{tot}[bulk] - \sum_i n_i\mu_i + q(E_V + E_F + \Delta V[D]), \quad (1)$$

where $E_{tot}[D(q)]$ is the total energy of the supercell containing the defect D in charge state q, E_{tot}[bulk] is the total energy in the same supercell without the defect, n_i is the atom number of the ith constituent, which has been added to ($n_i > 0$) or removed from ($n_i < 0$) the host material, and μ_i is its chemical potential. E_F is the Fermi level referenced to the VBM E_V of the bulk. The range of E_F is taken to be the band gap of the bulk. A correction term ΔV[D] is introduced in order to align the reference electrostatic potential in the charged defect supercell with that in the bulk. For the finite supercell calculation, a correction term E_{corr} is also needed due to the dispersion of the defect level, especially for the shallow level. It can be inferred from the energy difference between the highest occupied state at the Γ point and the average value at several special k points. The chemical potentials μ closely depend on the growth conditions and can be determined by,

$$\mu_{Al} + \mu_N = \mu_{AlN}, \quad (2)$$

$$\mu_{Ga} + \mu_N = \mu_{GaN}, \quad (3)$$

$$3\mu_{Mg} + 2\mu_N = \mu_{Mg_3N_2}, \quad (4)$$

$$\mu_N \le \mu_{N[N_2]}. \quad (5)$$

Because the group-III nitride semiconductors are usually grown under the N-rich and N-poor conditions[26,29,30], which directly determine the kind and concentration of defects in semiconductors, we thus consider these two limited cases to calculate the Mg acceptor formation energy. For the N-rich case, $\mu_N = \mu_{N[N_2]}$ (the energy of N in a N_2 molecule). Otherwise, for the N-poor case, $\mu_{Al(Ga)} = \mu_{Al(Ga)[bulk]}$, i.e., the energy of Al (Ga) in bulk Al (Ga). The Mg acceptor level $\varepsilon(0/-1)$, i.e., the activation energy, is defined as the E_F position where the charge states of $q = 0$ and -1 have equal formation energy and can be calculated from the following formula,

$$E_A = E_{tot}[D^-] - E_{tot}[D^0] - E_V - \Delta V[D] + E_{corr}. \quad (6)$$

Our calculated formation energies as a function of E_F are shown in Figure 2 for Mg_{Ga} in nanoscale $(AlN)_5/(GaN)_1$ SL, and Mg_{Al} and Mg_{Ga} in $Al_{0.83}Ga_{0.17}N$ uniform alloy under N-poor and -rich conditions. We can see from Figure 2 that the E^f of Mg^0 under p-type condition (E_F close to the VBM) is larger than that of Mg^{1-} under n-type condition (E_F close to the bottom of the conduction band). We thus can understand that the Mg acceptor concentration is low in thermodynamic equilibrium due to its large E^f in p-type $(AlN)_5/(GaN)_1$ SL and $Al_{0.83}Ga_{0.17}N$ alloy, which is consistent with the

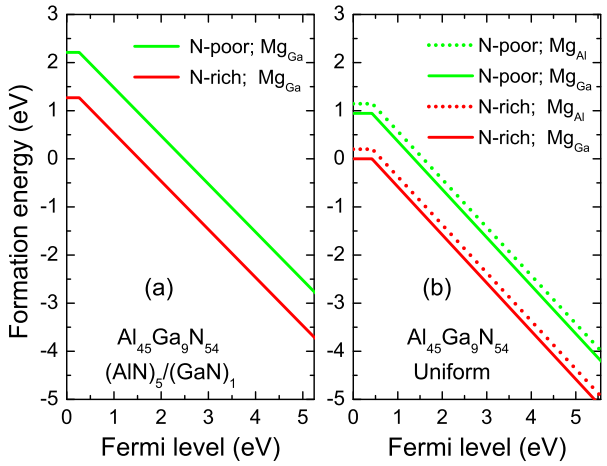

Figure 2 | Formation energy as a function of Fermi level E_F for (a) Mg_{Ga} in nanoscale $(AlN)_5/(GaN)_1$ SL and (b) Mg_{Al} and Mg_{Ga} in $Al_{0.83}Ga_{0.17}N$ uniform alloy under N-rich and –poor conditions. The zero of E_F corresponds to the VBM.

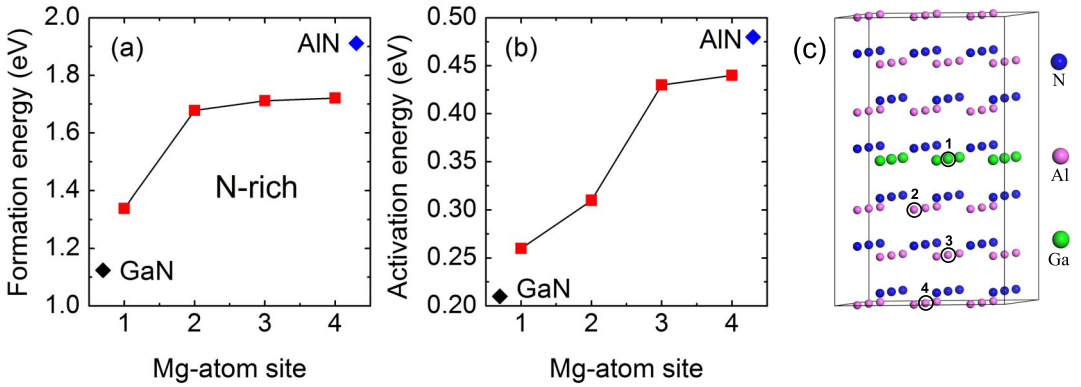

Figure 3 | Mg acceptor formation energy in neutral charge state (a) and its activation energy (b) as a function of Mg-atom site in $(AlN)_5/(GaN)_1$ SL. Here four special cation sites, surrounded with different next-nearest Ga atom numbers, are labeled in (c) for $3 \times 3 \times 3$ supercell. For the sake of comparison, Mg acceptor formation energy and activation energy in GaN and AlN are also presented. The lines are guides to the eyes.

previous experiment[31]. The formation energy as a function of E_F under N-poor is similar to that under N-rich. The E^f of Mg_{Ga} and Mg_{Al} decreases by 0.94 eV approximately from N-poor to -rich conditions because of the negative formation enthalpy of GaN and AlN. Moreover, we can see from Figure 2(a) that Mg_{Ga} in $(AlN)_5/(GaN)_1$ SL has two stable charge states, i.e., neutral 0 and −1, which induces a shallow acceptor level (0.26 eV). Figure 2(b) shows that E^f of Mg_{Ga} is about 0.20 eV lower than that of Mg_{Al} in $Al_{0.83}Ga_{0.17}N$ uniform alloy. The Mg atom thus tends to replace Ga atom other than Al atom. This can be attributed to the weak bond strength between Ga and N atoms compared to that between Al and N atoms.

The Mg atom can also substitute Al atom to form an acceptor in $(AlN)_5/(GaN)_1$ SL except for the aforementioned Mg_{Ga}. In order to know the preferable position of Mg^0 dopant, we further calculate its formation energy (see Figure 3(a)) for the chosen four special cation positions. The difference of sites 1–4 mainly concentrates on the nearest and NN neighbours of Mg, i.e., local structure around Mg atom (see Figure 3(c)). For the chosen four special positions, the NN Ga-atom numbers N_{Ga} are 6, 3, 0 and 0 from site 1 to 4, respectively. We can see from Figure 3(a) that the formation energy E^f increases monotonically from site 1 to 4 in $(AlN)_5/(GaN)_1$ SL, which is larger than E^f of Mg^0 in GaN and smaller than that in AlN, as it should be.

Table 1 | Comparison of Mg acceptor activation energy E_A (in unit of eV) with other calculations and experiments in wurtzite GaN, AlN and $Al_{0.83}Ga_{0.17}N$ uniform alloy

	This work	Other calc.	Expt.
GaN:Mg_{Ga}	0.21	0.26[a]	0.25[d]
		0.204[b]	0.208[e]
		0.198[c]	0.16[f]
AlN:Mg_{Al}	0.48	0.78[b]	0.50[f,i,k,l]
		0.58[g]	
		0.45[h]	
		0.40[i]	
AlGaN:Mg_{Ga}	0.44		0.4 ~ 0.5[f]
AlGaN:Mg_{Al}	0.44		0.4 ~ 0.5[f]

[a]HSE calculation from Ref. 32.
[b]Effective mass theory, Ref. 33.
[c]LDA calculation from Ref. 34.
[d]Ref. 35.
[e]Ref. 36.
[f]Ref. 9.
[g]Full-potential linearized augmented plane-wave (FPLAPW) with GGA-PBE, see Ref. 37.
[h]LDA calculation from Ref. 38.
[i]LDA calculation from Ref. 14.
[j]Ref. 17.
[k]DUV PL and Hall-effect measurements, see Ref. 39.
[l]DUV picosecond time-resolved PL spectroscopy, see Ref. 40.

The E^f rapidly increases from site 1 to 2, then slowly increases from site 2 to 4. This is because the Ga-N bond is weaker than the Al-N bond. We can conclude that Mg atom tends to occupy Ga site to form Mg_{Ga} acceptor in $(AlN)_5/(GaN)_1$ SL. This can be realized by means of Mg δ-doping technique, i.e., closing Al flow and leaving Ga and Mg flow[16].

We further calculate Mg acceptor activation energy E_A in GaN, AlN, and $Al_{0.83}Ga_{0.17}N$ uniform alloy (see Table 1). For the sake of comparison, some previous theoretical and experimental results are also given. We can see from Table 1 that our calculated E_A is 0.21 eV in GaN, which is within the range of well-accepted theoretical results (0.198–0.26 eV)[32–34] and experimental values (0.16–0.25 eV)[9,35,36]. For Mg dopant in AlN, excellent agreement of E_A (0.48 eV) with the previous theoretical calculations (0.40–0.78 eV)[14,33,37,38] and experiments (0.5 eV)[9,17,39,40] is also confirmed. This clearly indicates that our current calculations with the AM05 exchange-correlation (XC) functional[41] are accurate and reliable for the acceptor activation energy. Moreover, we calculate E_A of Mg_{Ga} and Mg_{Al} acceptors in $Al_{0.83}Ga_{0.17}N$ uniform alloy and find that they have equal E_A (0.44 eV) despite different cation sites occupied by Mg atom, which is in the range of the reported experimental values from 0.40 eV for Al-content $x = 0.7$ to 0.50 eV for $x = 1.0$[9]. It is worthwhile to note that, in spite of the Al-site or Ga-site occupied by Mg atom, E_A in $Al_{0.83}Ga_{0.17}N$ uniform alloy is always large and approaches the corresponding value of AlN. Therefore, it is extremely difficult to reduce Mg acceptor activation energy in Al-rich AlGaN. We will turn our attention to Mg dopant in $(AlN)_5/(GaN)_1$ SL substitution for $Al_{0.83}Ga_{0.17}N$ disorder alloy and seek a new way to reduce E_A in the following text.

Figure 3(b) shows our calculated Mg acceptor activation energies E_A in nanoscale $(AlN)_5/(GaN)_1$ SL as a function of Mg-atom position, which are in the range of 0.21 eV in GaN and 0.48 eV in AlN. We can see from Figure 3(b) that E_A in site 1 with the NN Ga-atom number $N_{Ga} = 6$ has its smallest value of 0.26 eV, which is very close to the Mg acceptor E_A in GaN. Then, E_A increases by 0.06 eV from site 1 to 2 with $N_{Ga} = 3$, and has a remarkable increase by 0.11 eV from site 2 to 3 ($N_{Ga} = 0$). The E_A keeps a constant approximately from site 3 to 4 ($N_{Ga} = 0$). These results clearly show that N_{Ga} or local structure of Mg atom has a significant influence on Mg acceptor E_A in SL. By increasing the NN Ga-atom number around Mg dopant, its activation energy E_A can be reduced remarkably. We further estimate hole concentration and find that it can reach to 10^{19} cm^{-3} in the SL at room temperature. This is extremely important and highly desired for the Al-rich AlGaN-based DUV optoelectronic devices. It is worthwhile to note that the hole concentration can be reduced due to the compensation of donors, such as nitrogen vacancies, which has not been considered in the above estimation. The concentration will

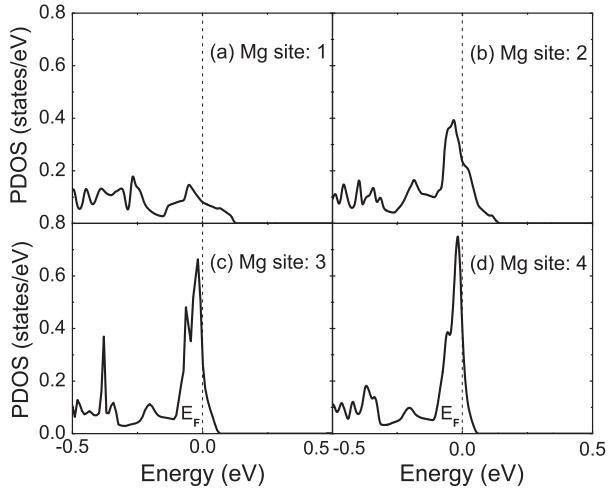

Figure 4 | The Mg PDOS near Fermi level E_F in *p*-type $(AlN)_5/(GaN)_1$ SL for different Mg doping-sites (see Figure 3(c)).

be further reduced owing to the high Mg acceptor activation energy if the Ga atoms are not restricted to a single atomic layer.

Discussion

Why does Mg acceptor activation energy sensitively depend on the local structure around Mg dopant and can be reduced significantly in nanoscale $(AlN)_5/(GaN)_1$ SL? According to the band offset explaination[42,43], Mg activation energy E_A is dominated by the position of the VBM state of the host material. The higher the VBM is, the lower the E_A is. In our current Mg doping calculations in $(AlN)_5/(GaN)_1$ SL, E_A has a significant variation with different Mg doping positions, whereas the VBM is always fixed. Obviously, the previous viewpoint cannot explain our results anymore. In order to have a deep understanding for the results of Figure 3(b), we further calculate the partial density of states (PDOS) of Mg atom near the Fermi energy in $(AlN)_5/(GaN)_1$ SL for different Mg doping positions (see Figure 4). We can find from Figure 4 that the localization of the Mg defect state sensitively depends on Mg site or local structure around it. The Mg impurity state changes markedly from the delocalized state to highly localized one from site 1 to 4 (see Figure 4(a–d)). According to the definition of shallow and deep levels in semiconductors[44], we know that the Mg_{Ga} acceptor level, corresponding to the delocalized state in site 1, is a shallow level. The acceptor level goes deeper from site 2 to 4 due to the strong localization of the Mg defect state. We thus can understand the results of Figure 3(b). Hence the Mg_{Ga} acceptor has the strongest delocalization, which results in the smallest acceptor activation energy in the SL.

Considering that the localization of Mg defect state is closely related to its local structure, we thus pay our attention to the relationship between the local structure and the localization of Mg defect state in order to explore the real physical origin of reducing Mg acceptor activation energy in nanoscale $(AlN)_5/(GaN)_1$ SL. Figure 5 shows the local structure around Mg acceptor, i.e., the Mg-centered tetrahedron, for the chosen four different Mg doping-sites. We find that the volumes V of Mg-centered tetrahedrons, indicating the average interaction strength between N and Mg atoms, are 4.317, 4.348, 4.360, and 4.374 Å^3 for Mg sites 1–4, respectively. The volume related to site 1 (4) is the smallest (largest). This is owing to the GaN-monolayer strong modulation effect, which is originated from the larger covalent radius of Ga atom than that of Al atom as the NN neighbors of Mg dopant. It is the variation of the local structure that leads to the difference of the interaction between N and Mg atoms, which directly modify the localization of the Mg defect state and Mg acceptor activation energy. The smaller V is, the stronger the N-Mg interaction is. The corresponding Mg defect state thus becomes more delocalization, and the activation energy is reduced due to the strong interaction between N and Mg atoms. We thus can understand that the local structure in Figure 5(a) has the smallest volume, the strongest N-Mg interaction, the most obvious delocalization of the Mg defect state (see Figure 4), and the smallest acceptor activation energy among the four different Mg doping-sites (see

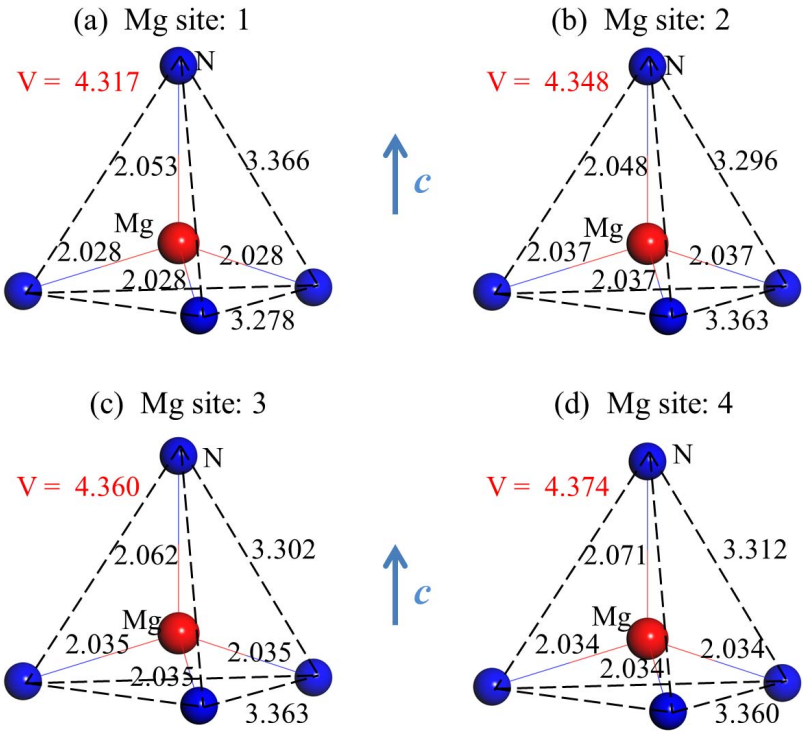

Figure 5 | Local-structure around Mg acceptor for the chosen four different Mg doping-sites (see Figure 3(c)). The calculated bond/edge length (in Å) and the tetrahedron volume V (in Å^3) are indicated.

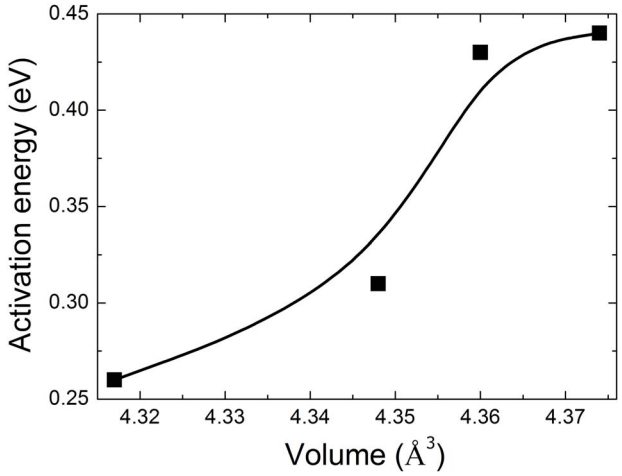

Figure 6 | Calculated Mg acceptor activation energy as a function of the Mg-centered tetrahedron volume (see Figure 5). The black line is the fitting curve to the calculated data points.

Figure 3(b)). It is note that the volume of the Mg-centered tetrahedron will increase if some Al atoms substitute Ga atoms in the single GaN layer due to the smaller covalent radius of Al atom, which increases the Mg acceptor activation energy.

In order to have an intuitive picture for the relationship between the Mg acceptor activation energy and its local structure, we give the E_A-V plot in Figure 6. It clearly shows that the smaller V is, the smaller the activation energy is. When the volume V has a slight increase from 4.317 to 4.374 Å^3 (~1.3%), E_A has a remarkable increase from 0.26 to 0.44 eV (~40.9%). Therefore, the local structure around Mg dopant plays a dominating role on the Mg acceptor activation energy. We thus open up a new way to reduce Mg acceptor activation energy in $Al_{0.83}Ga_{0.17}N$ disorder alloy substituted by nanoscale $(AlN)_5/(GaN)_1$ SL with Mg_{Ga} δ-doping. This picture is universal, which can be easily extended to other acceptor dopants in $(AlN)_m/(GaN)_n$ ($m > n$) SL and wide-gap semiconductors.

In summary, we calculate the formation energy and activation energy of Mg acceptor and investigate the relationship between the local structure around Mg atom and its activation energy in nanoscale $(AlN)_5/(GaN)_1$ SL substitution for $Al_{0.83}Ga_{0.17}N$ disorder alloy using first-principles calculations. We find that it is energetically more favourable for Mg atom to substitute Ga atom. The Mg acceptor activation energy sensitively depends on its local structure. The smaller the volume of the local structure is, the smaller the activation energy is. Our calculations show that Mg acceptor activation energy can be reduced significantly from 0.44 eV in $Al_{0.83}Ga_{0.17}N$ disorder alloy to 0.26 eV in $(AlN)_5/(GaN)_1$ SL by Mg_{Ga} δ-doping due to the GaN-monolayer strong modulation. The hole concentration can be significantly enhanced up to 10^{19} cm^{-3} in the SL at room temperature. Our results are vital for the realization of AlGaN-based DUV optoelectronic devices. We hope that this study would motivate further investigations in the near future.

Methods

Our first-principles calculations are based on the density functional theory with the generalized gradient approximation (GGA) functional and performed using the Vienna ab initio simulation package (VASP) code[45–48]. In our calculations, the AM05 XC functional[41] and projector augmented-wave (PAW) method are adopted to obtain accurate lattice constants[49]. We have built a Al-rich AlGaN supercell with $3 \times 3 \times 3$ wurtzite primitive cells. Two representative Ga distributions are considered. One is nanoscale $(AlN)_5/(GaN)_1$ SL with one GaN monolayer, and the other is $Al_{0.83}Ga_{0.17}N$ uniform alloy. The SL can be grown by metalorganic vapor phase epitaxy with sources of trimethylaluminum, trimethylgallium, and ammonia[27]. In order to minimize the strain, the supercell without Mg dopant is fully relaxed. Then the relaxed lattice vectors are fixed and the polarization effect is considered in our doping calculations. The N ($2s^2 2p^3$), Mg ($3s^2$), Al ($3s^2 3p^1$), and Ga ($3d^{10} 4s^2 4p^1$) are treated as valence electrons. The plane-wave basis set with a cutoff energy of 500 eV and the Monkhorst-Pack k-point grid[50] of $4 \times 4 \times 2$ have been checked carefully. In our current calculations, the total energy is converged to less than 10^{-5} eV. The maximum force is less than 0.02 eV/Å to guarantee that the stress is released completely. Based on these parameters, we calculate the lattice constant and valence band width (VBW) of GaN and AlN. Our calculated lattice constants are 3.18 (3.11) Å for a and 5.18 (4.98) Å for c and the VBW is 7.1 (6.0) eV for GaN (AlN), which are in excellent agreement with experiment[51].

Considering that the band gap is seriously underestimated in the usual GGA functional, we thus adopt the LDA-1/2 method[52,53] to improve our calculations, in which the half ionization is applied to the p-orbital of N atom and d-orbital of Ga atom. We choose the trimming parameter $CUT = 2.90$ (a.u.) and the power $n = 8$ for N atom, and 1.23 (a.u.) and 100 for Ga atom. This is because our calculated band gaps with these parameters are 3.51 and 6.01 eV for GaN and AlN, which are in good agreement with their experimental values. Our calculated band gaps are 5.24 and 5.56 eV for $(AlN)_5/(GaN)_1$ SL and $Al_{0.83}Ga_{0.17}N$ uniform alloy, respectively.

1. Allerman, A. A. *et al.* Growth and design of deep-UV (240–290 nm) light emitting diodes using AlGaN alloys. *J. Cryst. Growth* **272**, 227–241 (2004).
2. Zhang, J. P. *et al.* AlGaN-based 280 nm light-emitting diodes with continuous-wave power exceeding 1 mW at 25 mA. *Appl. Phys. Lett.* **85**, 5532–5534 (2004).
3. Asif Khan, M. AlGaN multiple quantum well based deep UV LEDs and their applications. *Phys. Status Solidi A* **203**, 1764–1770 (2006).
4. Al Tahtamouni, T. M., Sedhain, A., Lin, J. Y. & Jiang, H. X. Growth and photoluminescence studies of a-plane $AlN/Al_xGa_{1-x}N$ quantum wells. *Appl. Phys. Lett.* **90**, 221105 (2007).
5. Zhang, J. P. *et al.* AlGaN multiple-quantum-well-based, deep ultraviolet light-emitting diodes with significantly reduced long-wave emission. *Appl. Phys. Lett.* **83**, 3456–3458 (2003).
6. Collins, C. J. *et al.* Enhanced room-temperature luminescence efficiency through carrier localization in $Al_xGa_{1-x}N$ alloys. *Appl. Phys. Lett.* **86**, 031916 (2005).
7. Kneissl, M. *et al.* Advances in group III-nitride-based deep UV light-emitting diode technology. *Semicond. Sci. Technol.* **26**, 014036 (2011).
8. Gao, N. *et al.* Surface-plasmon-enhanced deep-UV light emitting diodes based on AlGaN multi-quantum wells. *Sci. Rep.* **2**, 816; DOI:10.1038/srep00816 (2012).
9. Pantha, B. N., Lin, J. Y. & Jiang, H. X. *High-Quality Al-Rich AlGaN Alloys* in *GaN and ZnO-Based Materials and Devices*, (ed. Pearton, S.) Ch. 2, 29–82 (Springer, 2012).
10. Simon, J., Protasenko, V., Lian, C., Xing, H. & Jena, D. Polarization-Induced Hole Doping in Wide-Band-Gap Uniaxial Semiconductor Heterostructures. *Science* **327**, 60–64 (2010).
11. Gao, L., Xie, F. & Yang, G. Numerical study of polarization-doped AlGaN ultraviolet light-emitting diodes. *Superlatt. Microstruct.* **71**, 1–6 (2014).
12. Al Tahtamouni, T. M., Lin, J. Y. & Jiang, H. X. Effects of Mg-doped AlN/AlGaN superlattices on properties of p-GaN contact layer and performance of deep ultraviolet light emitting diodes. *AIP Advances* **4**, 047122 (2014).
13. Aoyagi, Y., Takeuchi, M., Iwai, S. & Hirayama, H. High hole carrier concentration realized by alternative co-doping technique in metal organic chemical vapor deposition. *Appl. Phys. Lett.* **99**, 112110 (2011).
14. Wu, R. Q. *et al.* Enhancing hole concentration in AlN by Mg:O codoping: Ab initio study. *Phys. Rev. B* **77**, 073203 (2008).
15. Aoyagi, Y., Takeuchi, M., Iwai, S. & Hirayama, H. Formation of AlGaN and GaN epitaxial layer with high p-carrier concentration by pulse supply of source gases. *AIP Advances* **2**, 012177 (2012).
16. Nakarmi, M. L., Kim, K. H., Li, J., Lin, J. Y. & Jiang, H. X. Enhanced p-type conduction in GaN and AlGaN by Mg-δ-doping. *Appl. Phys. Lett.* **82**, 3041–3043 (2003).
17. Nakarmi, M. L. *et al.* Electrical and optical properties of Mg-doped $Al_{0.7}Ga_{0.3}N$ alloys. *Appl. Phys. Lett.* **86**, 092108 (2005).
18. Kinoshita, T., Obata, T., Yanagi, H. & Inoue, S. I. High p-type conduction in high-Al content Mg-doped AlGaN. *Appl. Phys. Lett.* **102**, 012105 (2013).
19. Nikishin, S. *et al.* Luminescence properties of $Al_xGa_{1-x}N$ ($0.4 < x < 0.5$)/$Al_yGa_{1-y}N$ ($0.6 < y \leq 1$) quantum structures grown by gas source molecular beam epitaxy. *Phys. Status Solidi C* **5**, 1852–1854 (2008).
20. O'Donnell, K. P., Martin, R. W. & Middleton, P. G. Origin of Luminescence from InGaN Diodes. *Phys. Rev. Lett.* **82**, 237–240 (1999).
21. Lemos, V. *et al.* Evidence for Phase-Separated Quantum Dots in Cubic InGaN Layers from Resonant Raman Scattering. *Phys. Rev. Lett.* **84**, 3666–3669 (2000).
22. Krestnikov, I. L. *et al.* Quantum dot origin of luminescence in InGaN-GaN structures. *Phys. Rev. B.* **66**, 155310 (2002).
23. Zvanut, M. E. *et al.* The effect of growth parameters on the Mg acceptor in $In_xGa_{1-x}N$:Mg and $Al_xGa_{1-x}N$:Mg. *Phys. Status Solidi C* **11**, 594–597 (2014).
24. Sampath, A. V. *et al.* Characterization of nanometer scale compositionally inhomogeneous AlGaN active regions on bulk AlN substrates. *Solid-State Electron.* **54**, 1130–1134 (2010).
25. Yang, W. H. *et al.* High density GaN/AlN quantum dots for deep UV LED with high quantum efficiency and temperature stability. *Sci. Rep.* **4**, 5166 (2014).
26. Gao, M. *et al.* Compositional modulation and optical emission in AlGaN epitaxial films. *J. Appl. Phys.* **100**, 103512 (2006).

27. Taniyasu, Y. & Kasu, M. Polarization property of deep-ultraviolet light emission from *C*-plane AlN/GaN short-period superlattices. *Appl. Phys. Lett.* **99**, 251112 (2011).
28. Van de Walle, C. G. & Neugebauer, J. First-principles calculations for defects and impurities: Applications to III-nitrides. *J. Appl. Phys.* **95**, 3851–3879 (2004).
29. Webster, R. F. *et al.* Indium Nitride and Indium Gallium Nitride layers grown on nanorods. *J. Phys.: Conf. Ser.* **471**, 012025 (2013).
30. Zhao, S. *et al.* p-Type InN Nanowires. *Nano Lett.* **13**, 5509–5513 (2013).
31. Castiglia, A., Carlin, J.-F. & Grandjean, N. Role of stable and metastable Mg–H complexes in *p*-type GaN for cw blue laser diodes. *Appl. Phys. Lett.* **98**, 213505 (2011).
32. Lyons, J. L., Janotti, A. & Van de Walle, C. G. Shallow versus Deep Nature of Mg Acceptors in Nitride Semiconductors. *Phys. Rev. Lett.* **108**, 156403 (2012).
33. Mireles, F. & Ulloa, S. E. Acceptor binding energies in GaN and AlN. *Phys. Rev. B* **58**, 3879–3887 (1998).
34. Wang, F., Li, J., Li, S.-S., Xia, J.-B. & Wei, S.-H. Mg acceptor energy levels in $Al_xIn_yGa_{1-x-y}N$ quaternary alloys: An approach to overcome the *p*-type doping bottleneck in nitrides. *Phys. Rev. B* **77**, 113202 (2008).
35. Strite, S. & Morkoç, H. GaN, AlN, and InN: A review. *J. Vac. Sci. Technol. B* **10**, 1237–1266 (1992).
36. Götz, W. *et al.* Hall-effect characterization of III–V nitride semiconductors for high efficiency light emitting diodes. *Mater. Sci. Eng., B* **59**, 211–217 (1999).
37. Zhang, Y., Liu, W. & Niu, H. Native defect properties and *p*-type doping efficiency in group-IIA doped *wurtzite* AlN. *Phys. Rev. B* **77**, 035201 (2008).
38. Fara, A., Bernardini, F. & Fiorentini, V. Theoretical evidence for the semi-insulating character of AlN. *J. Appl. Phys.* **85**, 2001–2003 (1999).
39. Nakarmi, M. L. *et al.* Correlation between optical and electrical properties of Mg-doped AlN epilayers. *Appl. Phys. Lett.* **89**, 152120 (2006).
40. Nam, K. B., Nakarmi, M. L., Li, J., Lin, J. Y. & Jiang, H. X. Mg acceptor level in AlN probed by deep ultraviolet photoluminescence. *Appl. Phys. Lett.* **83**, 878–880 (2003).
41. Armiento, R. & Mattsson, A. Functional designed to include surface effects in self-consistent density functional theory. *Phys. Rev. B* **72**, 085108 (2005).
42. Zhang, S. B., Wei, S.-H. & Zunger, A. A phenomenological model for systematization and prediction of doping limits in II–VI and I–III–VI2 compounds. *J. Appl. Phys.* **83**, 3192–3196 (1998).
43. Zhang, S. B., Wei, S.-H. & Zunger, A. Overcoming doping bottlenecks in semiconductors and wide-gap materials. *Physica B (Amsterdam)* **273**, 976–980 (1999).
44. Li, M.-F. *Modern Semiconductor Quantum Physics*. (World scientific 1995).
45. Kresse, G. & Hafner, J. Ab initio molecular dynamics for liquid metals. *Phys. Rev. B* **47**, 558–561 (1993).
46. Kresse, G. & Hafner, J. Ab initio molecular-dynamics simulation of the liquid-metal–amorphous-semiconductor transition in germanium. *Phys. Rev. B* **49**, 14251–14269 (1994).
47. Kresse, G. & Furthmüller, J. Efficient iterative schemes for ab Initio total-energy calculations using a plane-wave basis set. *Phys. Rev. B* **54**, 11169–11186 (1996).
48. Kresse, G. & Furthmüller, J. Efficiency of ab-initio total energy calculations for metals and semiconductors using a plane-wave basis set. *Comput. Mat. Sci.* **6**, 15–50 (1996).
49. de Carvalho, L. C., Schleife, A. & Bechstedt, F. Influence of exchange and correlation on structural and electronic properties of AlN, GaN, and InN polytypes. *Phys. Rev. B* **84**, 195105 (2011).
50. Monkhorst, H. J. & Pack, J. Special points for Brillouin-zone integrations. *Phys. Rev. B* **13**, 5188–5192 (1976).
51. Schulz, H. & Thiemann, K. H. Crystal structure refinement of AlN and GaN. *Solid State Commun.* **23**, 815–819 (1977).
52. Ferreira, L., Marques, M. & Teles, L. Approximation to density functional theory for the calculation of band gaps of semiconductors. *Phys. Rev. B* **78**, 125116 (2008).
53. Pelá, R. R. *et al.* Accurate band gaps of AlGaN, InGaN, and AlInN alloys calculations based on LDA-1/2 approach. *Appl. Phys. Lett.* **98**, 151907 (2011).

Acknowledgments

This work was supported by the National Basic Research Program of China (2012CB619304), and the National Natural Science Foundation of China (11474012, 11364030).

Author contributions

The idea was conceived by J.S. The calculation was performed by H.Z. The data analyses were performed by H.Z., J.S., M.Z., X.J., P.H. and Y.D. This manuscript was written by H.Z. and J.S. All authors reviewed this manuscript.

Additional information

Competing financial interests: The authors declare no competing financial interests.

How to cite this article: Zhong, H.-x. *et al.* Reducing Mg Acceptor Activation-Energy in $Al_{0.83}Ga_{0.17}N$ Disorder Alloy Substituted by Nanoscale $(AlN)_5/(GaN)_1$ Superlattice Using Mg_{Ga} δ-Doping: Mg Local-Structure Effect. *Sci. Rep.* **4**, 6710; DOI:10.1038/srep06710 (2014).